



### **Science Arts & Métiers (SAM)**

is an open access repository that collects the work of Arts et Métiers Institute of Technology researchers and makes it freely available over the web where possible.

This is an author-deposited version published in: <https://sam.ensam.eu>  
Handle ID: <http://hdl.handle.net/10985/15820>

#### **To cite this version :**

Maxim VAN DEN ABBEELE, Fan LI, Vincent POMERO, Dominique BONNEAU, Baptiste SANDOZ, Wafa SKALLI, Sébastien LAPORTE - A subject-specific biomechanical control model for the prediction of cervical spine muscle forces - Clinical Biomechanics - Vol. 51, p.58-66 - 2018

Any correspondence concerning this service should be sent to the repository

Administrator : [scienceouverte@ensam.eu](mailto:scienceouverte@ensam.eu)





## Science Arts & Métiers (SAM)

is an open access repository that collects the work of Arts et Métiers ParisTech researchers and makes it freely available over the web where possible.

This is an author-deposited version published in: <http://sam.ensam.eu>  
Handle ID: <http://hdl.handle.net/null>

### To cite this version :

Aliasghar A BEHNAMGHADER, Denis D NAJJAR, Alain IOST, Stéphane S BENAYOUN -  
Mechanical behavior study of plasma sprayed hydroxyapatite coatings onto Ti6Al4V substrates  
using scratch test - Materials Science Forum - Vol. 638-642, p.641-646 - 2010

Any correspondence concerning this service should be sent to the repository

Administrator : [archiveouverte@ensam.eu](mailto:archiveouverte@ensam.eu)

# Mechanical behavior study of plasma sprayed hydroxyapatite coatings onto Ti6Al4V substrates using scratch test

A. Behnamghader<sup>1, a</sup>, D. Najjar<sup>2, b</sup>, A. Iost<sup>2, c</sup> and S. Benayoun<sup>3, d</sup>

<sup>1</sup>Biomaterials laboratory, Materials and Energy Research Center, Alvand St, Argentine sq., PB 14155-4777, Teheran, Iran

<sup>2</sup> Arts et Metiers ParisTech, CNRS, LMPGM, 8 boulevard Louis XIV, 59046 Lille Cedex, France

<sup>3</sup>Laboratoire de Tribologie des Systèmes, CNRS, UMR 5513, Ecole de Centrale Lyon, 36 avenue Guy de Collongue, 69131 Ecully, France

<sup>a</sup>a-behnamghader@merc.ac.ir, <sup>b</sup>denis.najjar@lille.ensam.fr, <sup>c</sup>alain.iost@lille.ensam.fr, <sup>d</sup>stephane.benayoun@ec-lyon.fr

**Keywords:** Scratch test; Scanning electron microscopy; Plasma spraying; Hydroxyapatite; Titanium alloy.

**Abstract.** Mechanical behavior and fracture mechanisms of plasma sprayed hydroxyapatite coatings on Ti-6Al-4V substrate were assessed taking into consideration two variables: the coating thickness and the substrate roughness. The results show that the specimens having a substrate arithmetic average roughness parameter  $R_a = 2.29 \mu\text{m}$  is favorable with respect to  $R_a = 1.23 \mu\text{m}$ . For coating thickness above  $105 \mu\text{m}$ , cracks can be observed in the coating/substrate interface and the higher critical load  $P_{c2}$  (used generally in comparative evaluation of adherence) decreases. A  $90 \mu\text{m}$  coating thickness sprayed on a substrate having an arithmetic average roughness parameter  $R_a$  equal to  $2.29 \mu\text{m}$  seems to be the best compromise between microstructure, mechanical resistance (high critical loads and fairly good contact quality) and long term stability in the physiological medium (low dissolution rate) for an orthopedic application.

## Introduction

Hydroxyapatite (HAP) is actually used as a biomaterial for artificial bone, joints and roots, owing to its excellent osteoconductivity [1]. The use of HAP coating onto Ti-6Al-4V metallic substrate for fixation has been successfully applied and accepted clinically and plasma-spraying is currently the primary method used to produce commercially coated implants [1]. However, the most important limitation in the clinical application of HAP coating-based prosthesis is the weak coating/substrate adhesion that can induce mechanical failure at the interface [2-7]. The aim of this work was to investigate the failure mechanisms, especially cracking, during scratch test and to evaluate qualitatively the adhesion between a plasma sprayed porous HAP coating and Ti-6Al-4V substrate taking into account two coating/substrate variables: the substrate roughness and the coating thickness.

## Experimental procedure

HAP coatings with thickness varying from 50 to  $325 \mu\text{m}$  were deposited by air plasma spraying on 25 mm diameter and 25 mm long Ti-6Al-4V rods. Before thermal spraying, the Ti-6Al-4V samples were sand blasted in order to obtain a favorable surface for mechanical bonding in the coating/substrate interface. Two substrate surfaces with arithmetic average roughness parameters  $R_a$  equal to  $2.29 \mu\text{m}$  and  $1.23 \mu\text{m}$  were respectively studied. Absolute hardness was respectively 233 VHN for the substrate and 209 VHN for a  $120 \mu\text{m}$  thick coating [8]. Microstructure of coatings was studied by X-ray diffraction and secondary electron microscopy (SEM).

Scratch tests were performed in ambient air using a Micro Scratch Tester MST-CSEMEX with a Rockwell-C diamond stylus (conical angle,  $120^\circ$ ; tip radius, 0.2 mm). Normal load was continuously

increased from 0 to 30 N at a load rate of 10 N/min. The specimen was horizontally moved under the stylus with a scratching speed of 2 mm/min. In such experimental conditions, scratches were 6 mm length. Acoustic emission and frictional force were monitored versus applied load and the scratches were observed by optical and scanning electron microscopy to assess the coating failure mechanism with regard to the lower and higher critical loads recorded and denoted respectively  $P_{c1}$  and  $P_{c2}$  [9-11]. If the former is usually defined as the normal load at which microcracks initiate in the coating, the latter at which spalling occurs is usually used as a comparative value of coating adhesion [12].

## Results and discussion

**Microstructure.** In a preliminary study, the X-ray diffraction reveals that HAP is the principal phase of coatings [8]. SEM observations of the plasma-sprayed coatings reveal typical features presented in numerous other studies [13-17]. The as-sprayed coating surface is characterized by unmelted or partially melted particles, fully molten splats, pores and emerging cracks that propagate in the molten areas (Fig. 1a). A lamellar microstructure with an orientation closely parallel to the coating/substrate interface is observed on cross-sections (Fig. 1b).

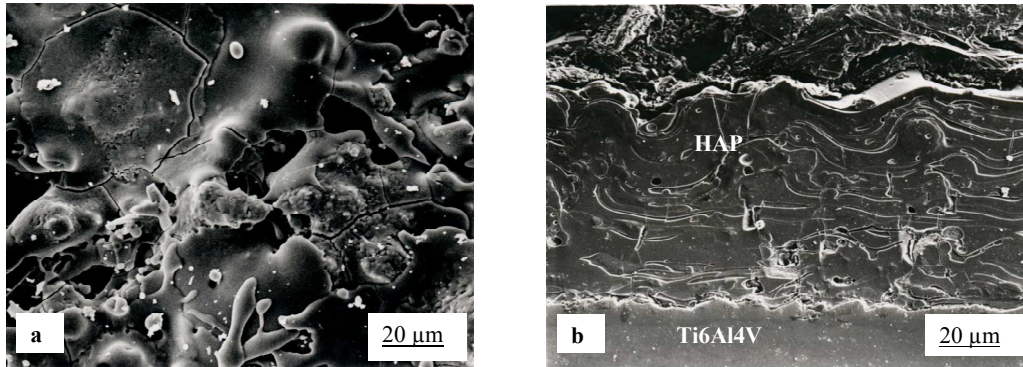


Figure 1: SEM micrographs showing: a) a typical top view of an HAP coating surface produced by air plasma spraying (coating thickness  $CT = 105 \mu\text{m}$ , substrate  $Ra = 2.29 \mu\text{m}$ ), b) a typical microstructure of the plasma-sprayed HAP through a coating cross-section ( $CT = 75 \mu\text{m}$ , substrate  $Ra = 1.23 \mu\text{m}$ ).

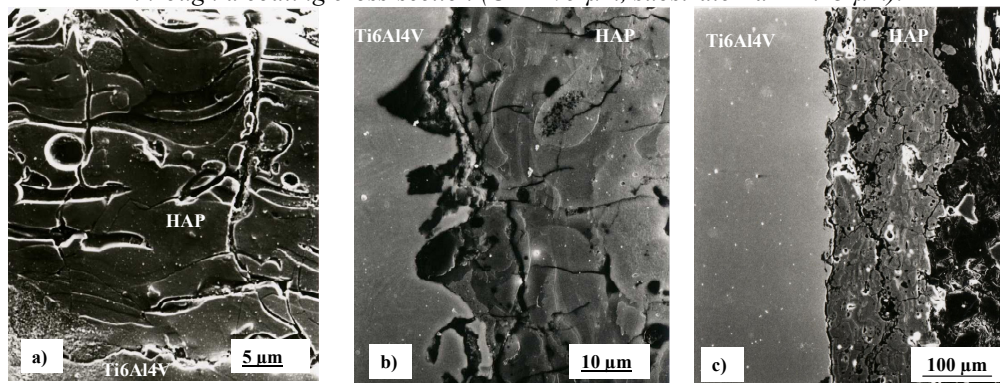


Figure 2: HAP coating cross sections showing: a) large perpendicular cracks emerging at the top surface ( $CT = 50 \mu\text{m}$ , substrate  $Ra = 1.23 \mu\text{m}$ ), b) fine perpendicular cracks ( $CT = 165 \mu\text{m}$ , substrate  $Ra = 2.29 \mu\text{m}$ ), c) interfacial and interlamellar cracks ( $CT = 150 \mu\text{m}$ , substrate  $Ra = 2.29 \mu\text{m}$ ).

The lamellar microstructure arising from the accumulation of the well-flattened molten splats contains also partially melted particles and various cracks. Some of the cracks are normal and others are parallel to the coating/substrate interface. Two kinds of normal cracks can be detected: large ones that emerge and open on the top surface of coating in the molten areas (Fig. 2a) and fine ones localized near the coating/substrate interface (Fig. 2b). It must be mentioned that the density of fine normal cracks increases when thickness of the coating increases. The parallel cracks are either localized in the interfaces of melted splats (interlamellar cracks) or in the interface between the coating and the substrate (interfacial cracks). For coatings deposited on the substrate having the

higher arithmetic average roughness parameter, cracks propagating in the interface are always detected when thickness is above  $105\ \mu\text{m}$  (Fig. 2c) and a good interfacial bonding is obtained when thickness is less or equal to  $90\ \mu\text{m}$ . Coatings deposited on the substrate having the lower arithmetic average roughness parameter  $R_a$  generally show the worse bonding quality with an increasing interfacial cracking propensity when thickness increases. It must be outlined that pores and cracks lower the coating mechanical performance on one hand but support the ingrowth of the tissue into the ceramic material on the other hand.

If the existence of pores can be related to entrapped gases, poorly melted particles and poor bonding between adjacent splats, cracking is the result of relaxation of the residual stresses developed in the ceramic coating during the deposition process [14-16, 18]. In this study, while the largest cracks normal to the coating/substrate interface are very probably the result of the relaxation of the residual tensile stresses [16], the parallel cracks are mainly promoted by in plane compressive stresses producing induced through-thickness tensile stresses [19, 20]. Finally, since the thermal expansion of HAP is above that of Ti-6Al-4V, the finest perpendicular cracks detected near the coating/substrate interface is thought to be the result of tensile stresses due to the thermal expansion mismatch. As mentioned by Yang et al. [20], the mechanism of residual stress generation and the impact of these residual stresses are so complicated that only few works are devoted to the quantitative prediction of the magnitude stress.

**Scratch testing and Scanning Electron Microscopy observations.** Whatever the substrate roughness, scratch tracks are not quite straight because the lack of contact between stylus and coating especially at the beginning of the mechanical tests. Microscopic evaluation shows that this fact is a consequence of coating roughness rather than substrate one. For each test, different events as cracking, progressive stylus penetration or instantaneous fracture of coating are encountered when the load increases. At the beginning of the test (low applied loads), a distribution of short cracks are detected in addition to the lack of contact between stylus and coating. When applied load increases, cracks become longer, the contact between stylus and coating becomes full and new features due to stylus crossing over pores are found.

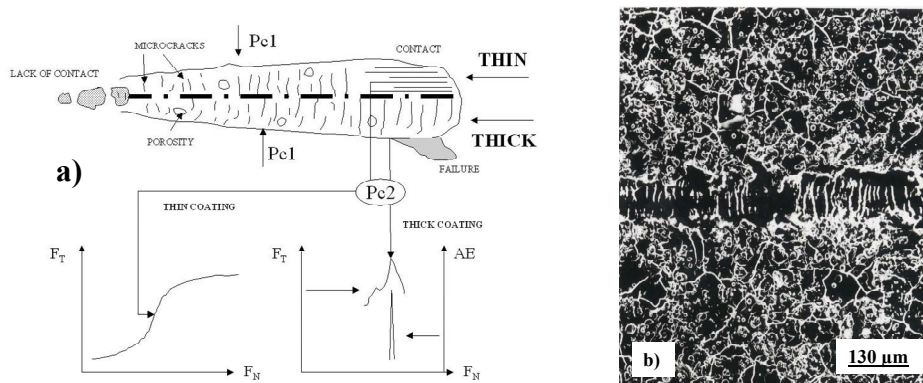


Figure 3: a) Synoptic of the events occurring on a typical scratch track under progressive loading and determination methodology of the critical loads for thick and thin coatings.  $P_{c1}$ : Normal load at which a microcrack reaches 50 % of the scratch track width.  $P_{c2}$ : Normal load ( $F_N$ ) corresponding either to the inflexion point of the frictional force ( $F_T$ ) graph for thin coating or to a sharp pulse on the acoustic emission signal (AE) combined with a sudden decrease of the frictional force for a thick coating, b) Example of microcracks formed during the scratch test in the range of applied loads near the  $P_{c1}$  value. This top view is related to the part of the graph indicated in Fig. 4.

An instantaneous adhesive spalling observed by visual inspection occurs generally before the contact between stylus and substrate, mainly in thick coating at high loads. This instantaneous spalling arises probably from the lateral crack propagation in the coating/substrate interface. On the other hand, for thin coatings, stylus can reach the substrate at intermediate loads without any instantaneous coating spalling ahead of the moving stylus. All these events are summarized on a synoptic of a typical scratch track in Fig. 3a. This figure presents also schematically how critical loads  $P_{c1}$  and  $P_{c2}$  were approximately determined.



Determination of the critical load  $P_{c1}$  for crack initiation was delicate. In fact, it is impossible to estimate directly and thoroughly  $P_{c1}$  considering only the graph of the frictional force or the graph of the acoustic emission because no significant change in these curves is observed (Fig. 4). Indeed, the frictional force does not change significantly for this critical load since cracks are produced behind stylus according to the Hertz theory [9]. As to the acoustic emission, microcracks initiating at  $P_{c1}$  produce only short single peaks hidden in the noisy background. The critical load  $P_{c1}$  was finally determined from numerous and attentive scanning electron microscopy observations of all coatings. These observations based on a comparative study of crack length revealed that the normal load value, for which a microcrack reaches a length of 50% of the scratch track width, may be a satisfactory criterion to evaluate  $P_{c1}$ . An example of the microcracks formed in a range of applied loads near the  $P_{c1}$  value is presented on Fig. 3b.

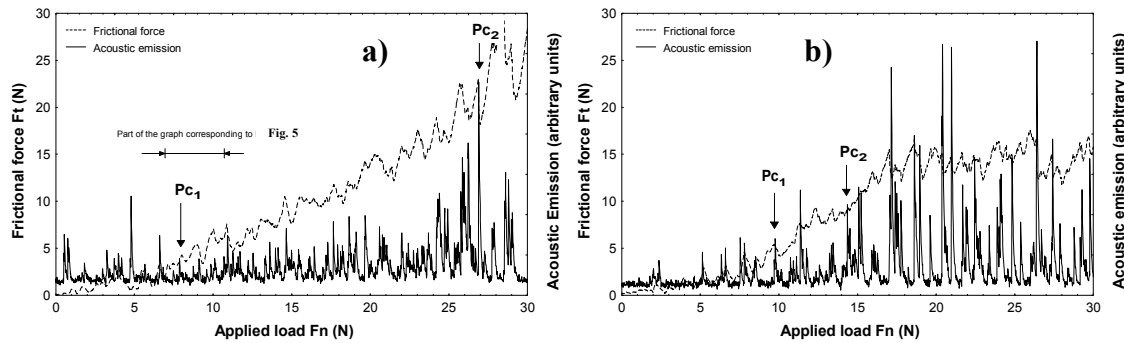


Figure 4: Typical acoustic emission and frictional force variations during a scratch test in the case of: a) a thick coating ( $CT = 105 \mu\text{m}$ , substrate  $Ra = 1.23 \mu\text{m}$ ), b) a thin coating ( $CT = 50 \mu\text{m}$ , substrate  $Ra = 1.23 \mu\text{m}$ ).

Critical load  $P_{c1}$  is plotted versus coating thickness in Fig. 5 for the two values of the arithmetic average roughness of the substrate considered in this study. Whatever the substrate roughness, the mean of this lower critical load increases with thickness. This result can be explained taking into consideration the observed increasing propensity of microcracking that occurs during the cooling process when coating thickness increases. Since microcracking is considered to be the main relaxation process of residual stresses during cooling of plasma sprayed coatings, short cracks due to the scratch testing may be expected to initiate more easily in the studied thin coatings. Moreover, for a given coating thickness, Fig. 5 reveals a trend showing that the substrate having the higher arithmetic average roughness parameter induces a better coating resistance to microcrack initiation since the mean of the lower critical loads recorded are higher than that of the substrate having the lower arithmetic average roughness parameter.

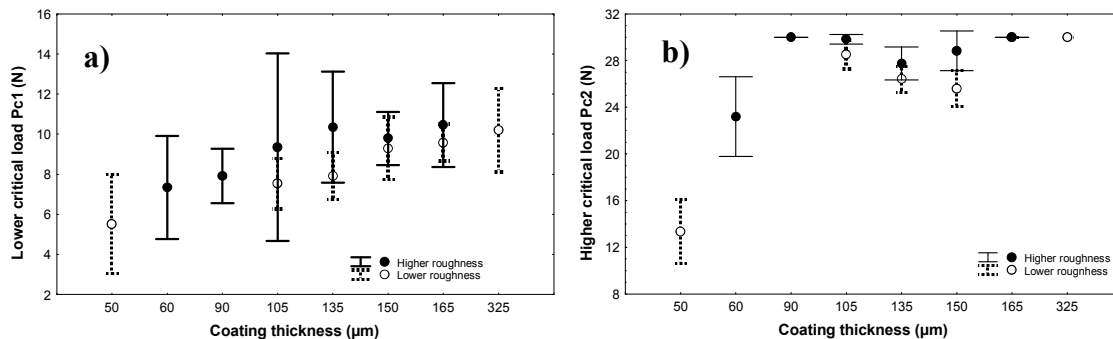


Figure 5: Lower (Left) and higher (Right) critical loads  $P_{c1}$  and the associated standard errors as a function of coating thickness for the two studied substrate roughness. Results correspond to 5 and 8 measurements whatever the experimental conditions.

Generally used in comparative evaluation of adherence, the higher critical load  $P_{c2}$  was estimated in this study as the normal load which corresponds either to the instantaneous spalling of the coating or to the contact beginning between the stylus and the substrate. For thick coatings, the observation of instantaneous spalling can be correlated with the occurrence of intense peaks on acoustic

---

emission curves combined simultaneously with a local sharp decrease of the frictional force at high loads (Fig. 4a). However, secondary pulses especially on acoustic emission curves may prevent to find the true peak and hence to estimate precisely  $P_{c2}$ . The secondary pulses appear at high loads and are mainly due to local coating failures that occur when the stylus interacts with pores or preexisting thermal cracks due to the plasma-spraying process. Sometimes, the stylus can cross over the largest defects associated with large and sharp discontinuities of surface topography resulting in significant sharp pulses on frictional force without significant effect on acoustic emission signal. The presence of such secondary pulses hampers the precise estimation of  $P_{c2}$  directly from the acoustic emission or the frictional force curves. This fact emphasizes the very usefulness of microscopic observations even if the lack of sufficient contrast of imaging between the coating and the substrate can be also an obstacle. In fact, the major problems encountered to estimate thoroughly  $P_{c2}$ , due either to the interaction between stylus and initial flaws generated during the plasma-spraying process in the coatings or to the lack of sufficient contrast of imaging, have been already mentioned by other authors [10, 12, 21].

Fig. 4b presents a typical graph of frictional force evolution and acoustic emission of a thin coating tested in this work. In this case, the higher critical load was assessed from microscopic observations and corresponds to the normal load for which the contact between the stylus and the substrate occurs. At first sight, it seems that the normal load value  $P_{c2}$  determined by these microscopic observations is not so far as the abscissa corresponding to the inflexion point on the frictional force graph. However, as mentioned by Stephanopoulos et al. [22], such a behavior is more representative of the interaction between the stylus and the substrate after the occurrence of contact rather than coating/substrate adhesion. As a consequence, it can be suspected that our experimental conditions of scratching may be no longer probing to predict adhesion of the HAP coatings which thickness is less or equal to 90  $\mu\text{m}$ .

$P_{c2}$  critical load values versus coating thickness are plotted in Fig. 5b for the two values of the arithmetic average roughness of the substrate considered in this study. It must be noted that it was not possible to determine the higher critical load for some of the thick coatings because of the upper experimental device loading limit (30 N). The higher  $P_{c2}$  values for specimens having the substrate roughness  $R_a$  of 2.29  $\mu\text{m}$  can be related to a better adherence. It must be outlined that the scratch test do not allow to obtain an absolute measure of coating adhesion because numerous extrinsic and intrinsic parameters influence the testing results [12].

## Conclusion

Many parameters corresponding to the testing conditions, coating/substrate interface and coating or substrate oneself play important roles on the determination of critical loads  $P_{c1}$  and  $P_{c2}$ . Therefore it is not simple to correlate scratch test data with coating/substrate adhesion energy and the higher critical load  $P_{c2}$  must be used only as a comparative value to characterize the coating adhesion. This study on HAP coatings emphasizes the interest in combining scratch testing with scanning electron microscopy observations. Indeed, such observations seems to be particularly more relevant than the evolution study of either the frictional force or the acoustic emission to estimate the lower critical load  $P_{c1}$  provided a criterion on microcrack length is fixed (50% of the scratch track width). Moreover, SEM observations give interesting informations on the significance of the higher critical load  $P_{c2}$  and put the experimenter on his guard against an abusive use of this macroscopic parameter. Indeed, for thin plasma-sprayed HAP coatings, the higher critical load may be more representative of the interaction between the stylus and the substrate after the occurrence of contact rather than coating adhesion.

In this work, scratch testing shows that a substrate roughness value of  $R_a = 2.29 \mu\text{m}$  is favorable with respect to  $R_a = 1.23 \mu\text{m}$ . The highest mechanical resistance (characterized by the  $P_{c2}$  values) is obtained for a coating thickness of 90  $\mu\text{m}$ , value below which the bonding quality between coating and substrate becomes excellent. Moreover, taking into account the biomedical aspects in HAP

prosthesis application, coating must be sufficiently thick because of HAP dissolution in the fluid environment [7]. Thus, a 90  $\mu\text{m}$  coating thickness sprayed on a substrate having an arithmetic average roughness parameter  $R_a$  equal to 2.29  $\mu\text{m}$  seems the best compromise between microstructure, mechanical resistance and long term stability in the physiological medium for an orthopedic application.

### Acknowledgments

The authors are pleased to acknowledge the CRITT Céramiques Fines de Maubeuge (France) for the elaboration of the plasma-sprayed coatings and Professor H. Migaud of the Centre Hospitalier Régional de Lille (France) for helpful discussions about the medical aspects of this work.

### References

- [1] H. Liang, B. Shi, A. Fairchild, T. Cale: *Vac.* 73 (2004), p. 317.
- [2] I.S. Lee, H.E Kim, S.Y. Kim: *Surf. Coat. Technol.* 131 (2000), p. 181.
- [3] L. Fu, K.A. Khor, J.P. Lim: *Surf. Coat. Technol.* 140 (2001), p. 263.
- [4] Z.S. Luo, F.Z. Cui, Q.L. Feng, H.D. Li, X.D. Zhu, M. Spector: *Surf. Coat. Technol.* 131 (2000), p. 192.
- [6] T.N. Kim, Q.L. Feng, Z.S. Luo, F.Z. Cui, J.O. Kim: *Surf. Coat. Technol.* 99 (1998), p. 20.
- [7] W. Suchanek, M. Yoshimura: *J. Mater. Res.* 13 (1998), p. 94.
- [8] A. Benhamghader, B. Farsadzadeh, D. Najjar, A. Iost: *Biomedical Engineering 2006* (IFMBE Proceedings, Malaysia 2006).
- [9] A. Darbeïda, J. Von Stebut: *Tribologie et Ingénierie des Surfaces*, (SIRPE, Paris, 1996).
- [10] J. Valli, U. Mäkelä, A. Matthews, V. Murawa: *J. Vac. Sci. Technol.* A3 (1985), p.2411.
- [11] A. Cavaleiro, M.T. Vieira: *Mater. Sci. Eng.* A140 (1991), p.631.
- [12] S.J. Bull, D.S. Rickerby: *Br. Ceram. Trans.* 88 (1989), p. 177.
- [13] C.Y. Yang, B.C. Wang, E. Chang, J.D. Wu: *J. Mater. Sci. Mater. Med.* 6 (1995), p. 249.
- [14] K.A. Khor, P. Cheang, Y. Wang: *JOM* 49 (1997), p. 51.
- [15] P. Filip, R. Melicharek, A.C. Kneissl, K. Mazanec: *Z. Metallkd.* 88 (1997), p. 131.
- [16] E. Park, R.A. Condrate, D.T. Hoelzer, G.S. Fischman, *J. Mater. Sci. Mater. Med.* 9 (1998), p. 643.
- [17] Y. Fu, A.W. Batchelor, Y. Wang, K.A. Khor: *Wear* 217 (1998), p. 132.
- [18] Y.C. Tsui, C. Doyle, T.W. Clyne: *Biomaterials* 19 (1998), p. 2015.
- [19] M. Levit, I. Grimberg, B.Z. Weiss: *Mater. Sci. Eng.* A206 (1996), p. 30.
- [20] Y.C. Yang, E. Chang: *Biomaterials* 22 (2001), p. 1827.
- [21] A.J. Perry: *Thin Solid Films* 107 (1983), p. 167 and *Thin Solid Films* 78 (1981), p. 77.
- [22] N. Stephanopoulos, V. Bellido-Gonzalez, B. Hopper, D.G. Teer: *Tribologie et Ingénierie des Surfaces*, (SIRPE, Paris, 1996).